EUR 12.e

EUROPEAN ATOMIC ENERGY COMMUNITY — EURATOM
Brussels (Belgium)

CENTRE D'ETUDE DE L'ENERGIE NUCLEAIRE — C.E.N.
Mol (Belgium)

MEASUREMENT OF THE THERMAL NEUTRON ABSORPTION CROSS SECTION OF BORON BY MEANS OF A TIME OF FLIGHT TECHNIQUE

by

A. DERUYTTER (CEN-SCK)
G. DEBUS, K. LAUER, H. MORET, A. PROSDOCIMI
(CBNM, Euratom)

MAY 1962

CENTRAL BUREAU FOR NUCLEAR MEASUREMENTS - EURATOM - GEEL
CENTRE D'ETUDE DE L'ENERGIE NUCLEAIRE - CEN - MOL

Report on Contract No 002.59.8 - AMPB

LEGAL NOTICE

This report can be obtained, at the price of Belgian Francs 30, from : PRESSES ACADEMIQUES EUROPEENNES, 98, chaussée de Charleroi, Brussels (Belgium).

Please remit payments :

— to BANQUE DE LA SOCIETE GENERALE (Agence Ma Campagne) account N° 964.558;

— to BELGIAN AMERICAN BANK and TRUST COMPANY — New York — account N° 121.86;

— to LLOYDS BANK (Foreign) Ltd, — 10 Moorgate — London E.C.2;

giving the reference : EUR 12.e — Measurement of the thermal neutron absorption cross-section of boron by means of a time of flight technique.

EUR 12.e

MEASUREMENT OF THE THERMAL NEUTRON ABSORPTION CROSS SECTION OF BORON BY MEANS OF A TIME OF FLIGHT TECHNIQUE BY A. DERUYTTER (CEN-SCK), G. DEBUS, K. LAUER, H. MORET, A. PROSDOCIMI (CBNM, EURATOM)

Central Bureau for Nuclear Measurements-EURATOM-Geel.
Centre d'Etude de l'Energie Nucleaire-CEN-Mol.
Report on contact n° 002.59.8 - AMPB.
May 1962 - pages 41 + fig. 10.

A precise determination of the neutron absorption cross-section of boron in the thermal energy region, 0.006 - 0.082 eV, has been undertaken by means of time-of-flight technique.

Two samples of deuterated boric acid solution in heavy water were measured, containing respectively 19.81 % and 96.51 % of B^{10}.

The following results were obtained (at 0.0253 eV) :

Sample n° 1 : $\sigma_a = (761 \pm 2)$b;

Sample n° 2 : $\sigma_a = (3703 \pm 9)$b;

from which the following values for the absorption cross section of B^{10} are respectively derived :

$\sigma_a (B^{10}) = (3840 \pm 11)$b;

$\sigma_a (B^{10}) = (3837 \pm 9)$b.

Their weighted mean is equal to (3838 ± 10)b.

EUR 12.e

MEASUREMENT OF THE THERMAL NEUTRON ABSORPTION CROSS SECTION OF BORON BY MEANS OF A TIME OF FLIGHT TECHNIQUE BY A. DERUYTTER (CEN-SCK), G. DEBUS, K. LAUER, H. MORET, A. PROSDOCIMI (CBNM, EURATOM)

Central Bureau for Nuclear Measurements-EURATOM-Geel.
Centre d'Etude de l'Energie Nucleaire-CEN-Mol.
Report on contract n° 002.59.8 - AMPB.
May 1962 - pages 41 + fig. 10.

A precise determination of the neutron absorption cross-section of boron in the thermal energy region, 0.006 - 0.082 eV, has been undertaken by means of time-of-flight technique.

Two samples of deuterated boric acid solution in heavy water were measured, containing respectively 19.81 % and 96.51 % of B^{10}.

The following results were obtained (at 0.0253 eV) :

Sample n° 1 : $\sigma_a = (761 \pm 2)$b;

Sample n° 2 : $\sigma_a = (3703 \pm 9)$b;

from which the following values for the absorption cross section of B^{10} are respectively derived :

$\sigma_a (B^{10}) = (3840 \pm 11)$b;

$\sigma_a (B^{10}) = (3837 \pm 9)$b.

Their weighted mean is equal to (3838 ± 10)b.

EUR 12.e

MEASUREMENT OF THE THERMAL NEUTRON ABSORPTION CROSS SECTION OF BORON BY MEANS OF A TIME OF FLIGHT TECHNIQUE BY A. DERUYTTER (CEN-SCK), G. DEBUS, K. LAUER, H. MORET, A. PROSDOCIMI (CBNM, EURATOM)

Central Bureau for Nuclear Measurements-EURATOM-Geel.
Centre d'Etude de l'Energie Nucleaire-CEN-Mol.
Report on contact n° 002.59.8 - AMPB.
May 1962 - pages 41 + fig. 10.

A precise determination of the neutron absorption cross-section of boron in the thermal energy region, 0.006 - 0.082 eV, has been undertaken by means of time-of-flight technique.

Two samples of deuterated boric acid solution in heavy water were measured, containing respectively 19.81 % and 96.51 % of B^{10}.

The following results were obtained (at 0.0253 eV) :

Sample n° 1 : $\sigma_a = (761 \pm 2)$b;

Sample n° 2 : $\sigma_a = (3703 \pm 9)$b;

from which the following values for the absorption cross section of B^{10} are respectively derived :

$\sigma_a (B^{10}) = (3840 \pm 11)$b;

$\sigma_a (B^{10}) = (3837 \pm 9)$b.

Their weighted mean is equal to (3838 ± 10)b.

EUR 12.e

EUROPEAN ATOMIC ENERGY COMMUNITY — EURATOM
Brussels (Belgium)

CENTRE D'ETUDE DE L'ENERGIE NUCLEAIRE — C.E.N.
Mol (Belgium)

MEASUREMENT OF THE THERMAL NEUTRON ABSORPTION CROSS SECTION OF BORON BY MEANS OF A TIME OF FLIGHT TECHNIQUE

by

A. DERUYTTER (CEN-SCK)
G. DEBUS, K. LAUER, H. MORET, A. PROSDOCIMI
(CBNM, Euratom)

MAY 1962

CENTRAL BUREAU FOR NUCLEAR MEASUREMENTS - EURATOM - GEEL
CENTRE D'ETUDE DE L'ENERGIE NUCLEAIRE - CEN - MOL

Report on Contract No 002.59.8 - AMPB

The present report describes a precision measurement of the absorption cross section of boron for thermal neutrons by a joint group of scientists from CEN-SCK, Mol, Belgium and from Euratom's Central Bureau for Nuclear Measurements, Geel, Belgium.

This programme was started at the end of 1959, at a time when the boron absorption cross-section values available presented discrepancies much larger than the errors quoted. Because of the importance of boron as a standard for neutron cross-section measurements, it was decided to try to improve the absorption cross-section measurement, as a supplement to the chemical and isotopic investigations on boron, already started in view of the establishment at the Central Bureau for Nuclear Measurements of a stock of standard boron.

Recent results on the boron absorption cross section have been obtained either for a neutron energy above 0.018 eV (ORNL-group) or with a crystal spectrometer (Columbia-group). It was felt that a measurement in an energy range centered around 0.025 eV and by a time-of-flight technique would be a useful addition to the available data.

I should like to thank the CEN-SCK-scientists, especially M. M. Nève de Mévergnies, head of the neutron physics department, for the very pleasant cooperation within the joint group.

J. SPAEPEN.

CONTENTS

KEY TO THE FIGURES

KEY TO THE TABLES

MEASUREMENT OF THE THERMAL NEUTRON ABSORPTION CROSS-SECTION OF BORON BY MEANS OF TIME OF FLIGHT TECHNIQUE

SUMMARY.

A precise determination of the neutron absorption cross-section of boron in the thermal energy region, 0.006 - 0.082 eV, has been undertaken by means of time-of-flight technique.

Two samples of deuterated boric acid solution in heavy water were measured, containing respectively 19.81 % and 96.51 % of B^{10}.

The following results were obtained (at 0.0253 eV) :

Sample n° 1 : $\sigma_a = (761 \pm 2)$b

Sample n° 2 : $\sigma_a = (3703 \pm 9)$b,

from which the following values for the absorption cross section of B^{10} are respectively derived :

$\sigma_a\ (B^{10}) = (3840 \pm 11)$b

$\sigma_a\ (B^{10}) = (3837 \pm 9)$b

Their weighted mean is equal to (3838 ± 10)b.

1. INTRODUCTION (*)

1.1 — Present status of the measurements.

The special importance of boron as a standard thermal neutron absorber is due both to the high absorption cross-section of its isotope of mass 10 in the reaction B^{10} (n, α) Li^7 and to its rigorous $1/\sqrt{E}$ behaviour versus the energy E of neutrons, a phenomenon which has been checked up to values of the order of 10^4 eV.

About 20 % of B^{10} is present in the natural element with fluctuations generally attributed to the geographical origin of the ore ; thus, mention of the origin should always be made in the case of "natural" boron.

The measuring procedures applied up to now consist, in general, of neutron transmission measurements, applying either time-of-flight methods (chopper and pulsed accelerators) or using monochromatic neutrons (crystal spectrometer). Some measuring procedures were based on the mean life of neutrons pulsed in an absorbent diffuser ; some others, applying the pile-oscillator method, made it possible to draw comparisons between various boron samples. Measurements of the mean life of neutrons, although more complicated from the standpoint of interpretation, give the absorption cross-section, whereas transmission measurements, being directly related to the total cross-section, require that the scattering cross-section is known.

(*) A. Prosdocimi, Euratom.

Table I gives for natural boron and its isotope B^{10} a complete and up-to-date picture of the results either published by other experimenters or obtained in the course of this investigation, expressed in terms of the absorption cross-section for 2,200 m/s neutrons (or with an energy of 0.0253 eV).

Before proceeding to a comparative analysis, a special remark should be made about the isotopic ratio of B^{10} to B^{11} in natural boron. In fact, the value of the absorption cross-section becomes significant only when such a parameter as can be obtained by means of mass-spectrometric determination is considered.

The main feature of the measurements made up to 1958 was that they were, in scope, restricted to natural boron, stocks of which had been prepared previously in various laboratories, and intended to carry out comparative measurements of the various stocks available. Determination of the isotopic ratio of B^{10} were carried out separately on the whole stock but not during each cross-section measurement.

It was thus ascertained that standard ANL - BNL boron from California contained (19.8 $\pm$ 0.2) % of B^{10}, ref. 11 and 15. For other boron supplies, the absorption cross-section ratios were found to be as follows :

Harwel/ANL-BNL	= 1.012 $\pm$ 0.003	ref. 4 and 16
Oxford/Harwell	= 1.001 $\pm$ 0.003	ref. 6
Stockholm/ANL-BNL	= 0.997 $\pm$ 0.007	ref. 9

A different trend noticeable in the recent measurements, made from 1960 onwards, consisted in determining the isotopic ratio of every sample subjected to neutron transmission, affording the possibility of utilizing samples with a higher B^{10} enrichment. Accordingly, the aim in view is now to arrive at a conclusive determination of the absorption cross-section of isotope B^{10} and to make the definition of the various boron standards either available or being established dependent upon the determination of their isotopic ratio. It is the desire to achieve this purpose which forms the basis of the experiment described in this report. The values of σ_A normalized for B^{10} and energy 0.0253 eV have thus been determined and are given in Table I for the purpose of comparison only.

1.2 — Purpose of the measurement.

If a comparison is made between the various values obtained for the thermal absorption cross-section of the so-called "natural boron", taking account of their respective statistical deviations (Fig. 1), the differences observed among them are not always justified by the level of accuracy attained during the measurements. These differences should be attributed to the presence of systematic errors which cannot always be clearly singled out or evaluated. It is with the main purpose of minimizing the causes of systematic error that we have resumed boron cross-section measurements, being particularly careful to achieve the same degree of accuracy in all the experimental steps contributing to the final result. It was necessary to cut down to essentials the data to be taken into account in the earlier works of previous research workers.

The essential factors affecting the accuracy of the results were as follows :—

— measurement of B^{10} isotopic ratio using a mass-spectrometer ; this measurement should be made with the same boron material as used for the experiment ;

— measurement of the boron content by chemical analysis, ascertaining at the same time its degree of chemical purity, in particular with respect to high neutron cross-section elements ;

— defining both the uniform thickness of the absorbent sample subjected to neutron transmission, this being obtained by accurate selection of materials, and the shape and dimensions of the container ;

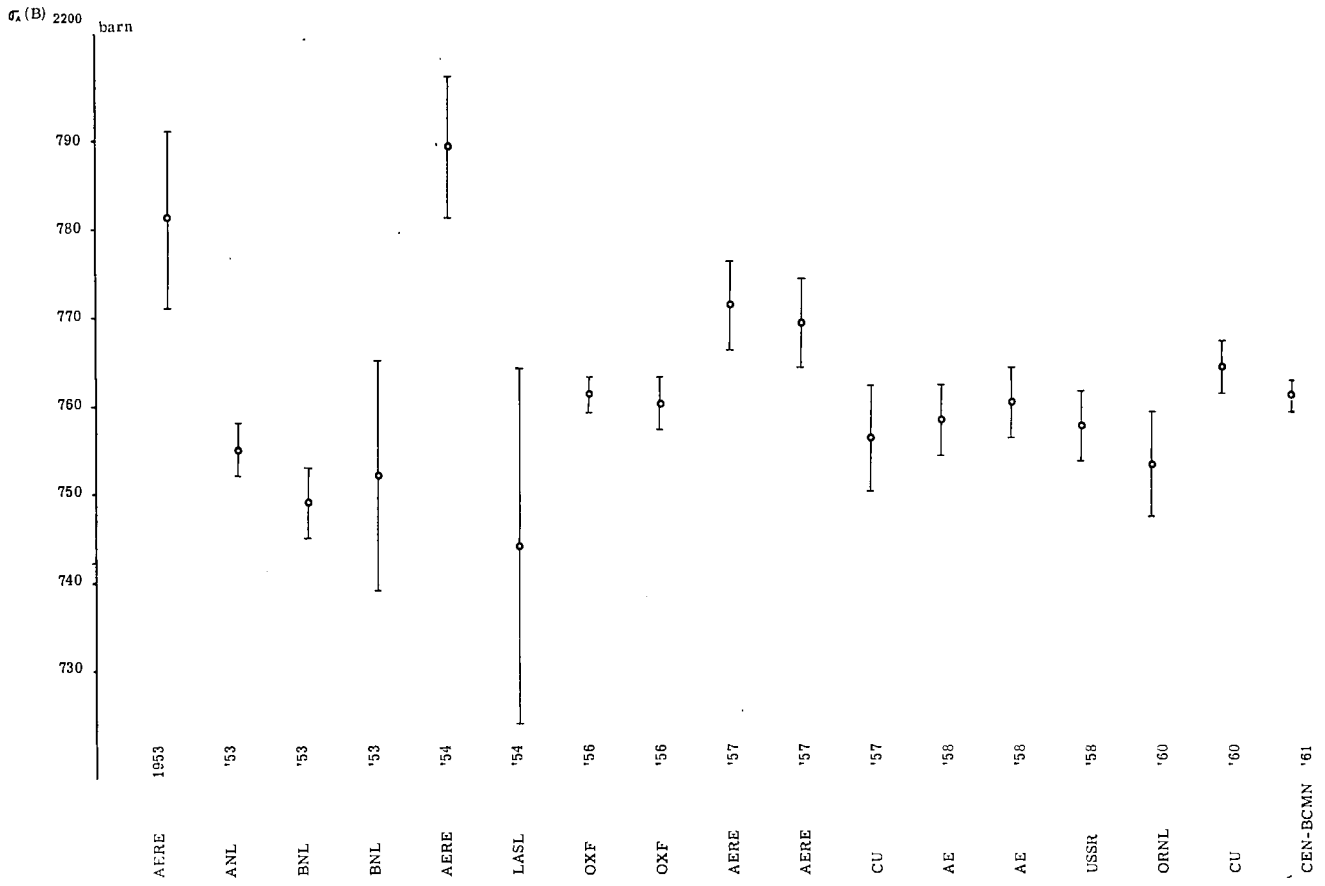

FIG. 1. — Present status of the thermal cross-section of natural B.

— establishing as neutron transmission of the boron sample a suitable value to be calculated on the basis of results selected on account of their statistical reliability and producing a high count likely to reduce the statistical error inherent in the measurement.

In the course of the experiment, many other precautions proved necessary, some of the most important of which were :

— elimination from the boron material of any trace of hydrogen ; this was achieved by using deuterated compounds only, and performing all handling operations in controlled atmosphere ;

— use of boron with high B^{10} enrichment in order to render negligible other sections of secondary importance in relation to the predominant value of σ_A (B^{10}) ;

— direct measurement of the transmission of the heavy water used as solvent in the preparation of the boron in order to correct for the effects of any density variation in the B_2O_3 solutions ;

— integral monitoring of the neutron beam in order to offset any intensity fluctuation of the neutron flux ;

— alternate cycle exposure of the samples to the neutron beam in order to offset the long-term drift to which the experimental conditions could be subject ;

— strictly accurate re-positioning of the sample in the neutron beam by means of an automatic device ;

— break-down into sub-totals of the count of the neutrons transmitted so as to check the statistical distribution of the measurements.

1.3 — Experimental method.

The measuring procedure followed was based on the transmission of a collimated neutron beam through a test specimen of uniform thickness d placed in the direction of the beam and made of a material with a total macroscopic cross-section Σ_T. As a result of being transmitted through the test specimen, the neutron beam of intensity I_o is attenuated to an intensity I according to the relation

$$I = I_0 \exp (- d \Sigma_T) \qquad [1]$$

In order to obtain a homogeneous distribution of the boron atoms in the specimen, the boron is utilized in the form of a B_2O_3 — heavy water solution kept in pure quartz containers with flat parallel walls. In these conditions, and with a container wall thickness δ, the neutron beam attenuation is :

$$I = I_0 \exp [-d \Sigma_T (B_2O_3) - d \Sigma_T (D_2O) - \delta \Sigma_T (SiO_2)] \qquad [2]$$

It is enough, then, to repeat the transmission measurement with the same container, filled this time with heavy water only,

$$I' = I_0 \exp [-d \Sigma_T (D_2O) - \delta \Sigma_T (SiO_2)] \qquad [3]$$

to derive from [2] and [3] the macroscopic cross-section of B_2O_3,

$$\Sigma_T (B_2O_3) = 1/d \cdot \ln (I'/I). \qquad [4]$$

In turn, the B_2O_3 total macroscopic cross-section is composed of the following terms, $N(B_2O_3)$ being the number of molecules per unit of volume.

$$\Sigma_T = N (B_2O_3) [2\sigma_A (B) + 2\sigma_S (B) + 3\sigma_T (O)] \qquad [5]$$

in wich

σ_A is the absorption microscopic cross-section
σ_S is the scattering microscopic cross-section
σ_T is the total microscopic cross-section.

The numerical values of the individual terms are, according to the current bibliographical references (ref. 17), given in "barn" units (i.e., 10^{-24} cm^2) and at the energy $E_0 = 0.0253$ eV,

Atom	σ_A	σ_S	σ_T
B^{10}	3848 ± 38	4.0 ± 0.5	—
B^{11}	0.005 ± 0.003	4.4 ± 0.3	—
O	—	—	4.24 ± 0.02

As in the present experiment the measurable quantity is that given between brackets in [5], it was necessary, in order to determine σ_A (B), to make a hypothesis on the remainning terms. In line with refs. 7 and 18, it was assumed that.

$$2\sigma_S \text{ (B)} + 3\sigma_T \text{ (O)} = 21 \text{ barns} \qquad [6]$$

The contribution of these terms to σ_T (B_2O_3) amounts to 1.3 % in the case of natural boron and to 0.3 % in the case of boron with 96 % B^{10} enrichment, so that any uncertainty involved cannot appreciably influence the results.

The transmission experiment was performed at the same time and in identical experimental conditions on 4 samples held in identical quartz cells :

a) 1.67 % solution of B_2O_3 in heavy water, (19.8 % of B^{10}) ;
b) 0.38 % solution of B_2O_3 in heavy water, (96.5 % of B^{10}) ;
c) heavy water, (compensation sample) ;
d) helium gas, (compensation sample).

From relative comparisons, the following measurements can be obtained :

a/c — total cross-section of B_2O_3 with 19.8 % of B^{10} enrichment ;
b/c — total cross-section of B_2O_3 with 96.5 % of B^{10} enrichment ;
c/d — total cross-section of heavy water.

This latter factor is designed to introduce the density correction as described in chapter 4.

The neutron beam was provided by the thermal column of the BR-1 reactor at Mol (power 4 MW), which has a Maxwellian spectrum with a characteristic temperature of 58° C.

Given the dependence of σ_A (B) on the neutron energy, the "time-of-flight" technique was applied to the transmission measurement using a thermal neutron chopper and a multi-channel analyser both of wich are described in chap. 3.

Two series of measurements, each one over 25 channels, covered the following energy ranges :

0.006 — 0.027 eV ; series "K" ;
0.013 — 0.082 eV ; series "L" ;

they were made to overlap at the conventional thermal energy of 0.0253 eV.

The value of σ_A (B) for neutrons of velocity 2,200 m/s is derived from the assumption that the 1/v law applies to boron within the energy range investigated. In other words, according to this hypothesis, the quantity.

$$K = \sigma_A \text{ (B)}/\tau = [\sigma_T \text{ (B_2O_3)} - 21 \text{ barns}]/2\tau \qquad [7]$$

should be independent of the energy (or of the time-of-flight τ). After having established the maintenance of such uniformity within the limits of the statistical deviations inherent in single measurements, we may finally obtain :

$$\sigma_A \text{ (B)}_{2200} = K \cdot \tau_{2200} \qquad [8]$$

2. SAMPLE PREPARATION

2.1 — Boron sample preparation (*).

2.1.1 — *Preparation of natural boron solution.*

As raw material, we used boric anhydride (a 5 kg batch of pure anhydride Merck, p. A.) supplied to us with the following analysis report :

B_2O_3 content :	99.4 %
Desiccation loss :	0.32 %
Chloride (Cl) :	approx. 0.0003 %
Sulphate (SO_4) :	approx. 0.003 %
Silicate (SiO_2) :	approx. 0.0008 %
Phosphate (PO_4) :	approx. 0.0005 %
Copper (Cu) :	approx. 0.00006 %
Lead and Zinc (as lead) :	approx. 0.0005 %
Iron (Fe) :	approx. 0.00007 %
Calcium (Ca) :	less than 0.001 %
Arsenic (As) :	practically free
Water :	maximum 0.32% (eliminated through desiccation)

An aliquot part of the Merck boric anhydride was oven-dried at 800-900° for about 6 hours in a platinum capsule to produce an anhydride, the water content of which was assumed to be of the order of 0.1 %. It was then dissolved in hot heavy water. After cooling down to approximately 0° C, the re-crystallized product was collected on a Gooch filter. The resulting chemical compound, corresponding to the formula B_2O_3, x H_2O, y D_2O was then exposed for 8 hours in an exsiccator to a dry nitrogen stream at 20°C to dehydrate it to a compound intermediate between D_3BO_3 and DBO_2. This compound contained negligible traces of H_3BO_3 + HBO_2, and has dissolved in heavy water to obtain a solution containing about 2 % of B_2O_3. Quartz containers were used for all handling operations and all operation performed in a dry base.

2.1.2 — *Preparation of the enriched boron solution.*

The B^{10} enriched compound was supplied by the Oak Ridge National Laboratory in the form of boric acid. It was dried at 20° C for 4 hours in an exsiccator in a dry nitrogen stream, re-crystallized from its heavy-water solution and dried again for 8 hours in a dry nitrogen stream. The product obtained, which corresponded to a formula identical to the one given for the natural boron product, was then dissolved in heavy water to obtain a solution containing approximately 0.5 % of B_2O_3. As in the first case, all the handling operations were carried out in quartz containers in a dry-box.

2.1.3 — *Checking of purified product.*

Both spectrum and chemical analysis confirmed the data given in the supplier's analysis report, demonstrating the absence in both natural and enriched boron compounds of harmful quantities of elements having high neutron cross-sections.

(*) K. F. Lauer, Euratom.

2.2 — Boron content determination (*).

The two solutions referred to above were titrated to determine their exact boric acid contents. The titration method used was based on the neutralization by sodium hydroxide of the highly acidity on boric acid-mannitol complex ; the end points of the reaction were detected by an accurate potentiometric method, (ref. 19).

By this method, the end point is localised by recording in the neighbourhood of the end point the derivative of succesive potential changes resulting from successive additions of very small quantities of NaOH(0,1n) of the order of 0.015 ml.

The total quantity of 0,1n NaOH used for titrating on known weight of H_3BO_3 solution is given by the volume dispensed between the first end point, corresponding to the neutralization of a few drops of hydrochloric acid added to the medium in the presence of the boric acid at the start of titration, and the end point corresponding to the final neutralization point of the boric acid after mannitol addition.

The normality of the NaOH solution was accurately determined by standardization with : *a*) HCl [concentration determined by gravimetric analysis (AgCl)], *b*) Potassium and phtalate (NBS) and benzoic acid (NBS).

On the other hand, the titration method was found to be in agreement within 0,04 % with the gravimetric analysis method used to determine the boric acid by weight [calcium borate] (ref. 20), this is less then the standard deviation (95 % security) of 0.045 % of the gravimetric method.

The results obtained were calculated by using the evaluation of the molecular weight of boric anhydride, the atomic weight of boron derived from its isotopic composition determined by mass spectrometry. The results are given in grams of boric anhydride per 100 g. of solution.

The various data regarding the solutions have been grouped in the following table :

	Natural Boron	*Enriched Boron*
Isotopic composition as shown by the mass spectrometry laboratory	% B^{10}=19.81 ± 0.02	% B^{01}=96.515 ± 0.013
Molecular weight of boric anhydride calculated on the basis of the isotopic content	69.6040 ± 0.0004	68.0696 ± 0.0002
Concentration of the solution in g. of B_2O_3 per 100 g. of solution	1.67712 ± 0.00018	0.38591 ± 0.00011

2.3 — Mass spectrometric determination (**).

A 60° deflection, 12 inch radius mass spectrometer was used for the isotopic analysis. The filaments for the triple filament source were fabricated of tantalum ribbon (0.0035 mm. x 0.7 mm.). These filaments were mounted on kovar terminals. A few drops of a concentrated solution of HBO_3 — NaOH mixture were loaded on the side filaments and evaporated to dryness in air. After mounting the filaments in the ion source the mass spectrometer was evacuated to $2 \cdot 10^{-6}$ mm Hg or better.

The filaments were heated by means of a d.c. electric current and $Na_2BO_2^+$ ions were obtained. On the recorded spectrum the $Na_2B^{11}O_2^+$ peak was corrected by — 0.074 % of the $Na_2B^{10}O_2^+$ peak (correction necssary for the contribution of the ion $Na_2B^{10}O^{16}O^{17}$ to the $Na_2B^{11}O^{16}O^{16}$ peak).

(*) K. F. Lauer, Euratom.
(**) G. Debus, Euratom.

Focussing of the two masses was obtained by a constant acceleration voltage (7000 V) and magnetic scanning.

The isotopic composition of a sample of normal boron was determined by measuring twenty loadings (each of 10 scans or more).

The final results were :

B^{10} : (19.81 ± 0.04) % (95 % probability for the standard deviation of the mean);

B^{11} : (80.19 ± 0.04) %.

A sample of enriched boron was measured (14 loadings of 10 scans or more).

The result was :

B^{10} : (96.515 ± 0.022) % (95 % prob. of stand. dev. of mean) ;

B^{11} : (3.485 ± 0.022) %.

A small amount of mass discrimination may influence the absolute value of these results. This mass discrimination is presently being investigated.

2.4 — Samples specifications (*).

2.4.1 — *Heavy water and solution densities.*

A batch of heavy water was completely distilled in a vacuum distillation apparatus, the first and last fraction being collected in a big flask, while the middle fraction was collected in a glass test tube containing a calibrated float made in fused quartz. Handling and distillation were performed in a special dry-box with a relative humidity better than 5 %. In order to carry out a density measurement the test tube was transferred to a high precision thermostat. The temperature is adjusted to a value at which the float is in kinetic equilibrium with the surrounding liquid, i.e. the densities of liquid and float are equal. From this temperature the density of D_2O at 25° C is derived by means of the known density of the float (ref. 21),

$$\rho_0 \ (25^\circ C) = 1.104485 \ g/cm^3.$$

To determine the densities of the natural and enriched boric acid solutions the filling tube of the cells were provided with a reference mark. By weighing the cells empty and filled with distilled water the volume capacity of each cell was measured. After the filling procedure the cells were weighed again. From these values the densities were then calculated.

Cell n°	*Filling*	*Density at 25° C*
3	He	—
4	D_2O	(1.104485 ± 0.000001) g/cm³
1	nat. boron solut.	(1.1162 ± 0.0001) »
6	enr. boron solut.	(1.1072 ± 0.0001) »

2.4.2 — *Measuring cells.*

The cells (Fig. 2), are made of fused quartz. The diameter and cell length d are 52 and 20 mm respectively. The cell length was specified with an accuracy of + 0.010 mm. These dimen-

(*) H. Moret, Euratom.

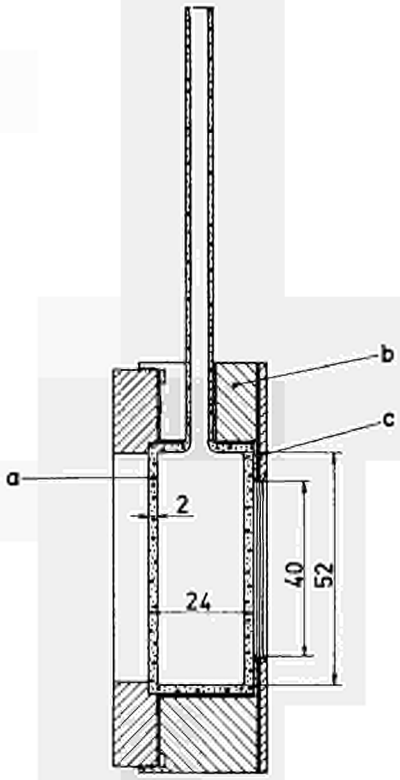

FIG. 2. — Measuring cell and neutron diaphragm.
a — Quartz cell.
b — Perspex holder.
c — Cadmium window.

sions could be determined with a method specially designed for this purpose : steel balls were dropped into the cells and magnetically clamped against the inner sides of the windows ; by means of a measuring microscope the distance between the balls was measured. From this the cell lengths and their uniformity could be determined with an accuracy of $\pm$ 5 μ (ref. 22). From the topography of the cells, the average cell lengths were calculated. Over a central area of 40 mm diameter the maximum deviations from the average value are smaller than $\pm$ 10 μ. The cell lengths and the thicknesses of the windows result :

Cell n°	*Cell length*	*Total thickness of the two windows*
3	(2.005 $\pm$ 0.001) cm	(0.395 $\pm$ 0.002) cm
4	(2.004 $\pm$ 0.001) »	(0.390 $\pm$ 0.002) »
1	(2.003 $\pm$ 0.001) »	(0.393 $\pm$ 0.001) »
6	(2.005 $\pm$ 0.001) »	(0.397 $\pm$ 0.002) »

(from BCMN Certificate E—39)

The vacuum tightness of the cells has been checked too. The filling of the cell was carried out in the controlled atmosphere of the dry-box. All the necessary equipment was

left in the dry-box during 24 hours. Then solution was transferred from the flask into the cells by means of hypodermic syringes. The fourth cell was flushed and filled with helium. After careful removal of air bubbles all the sample cells were sealed with a plastic cap.

2.4.3 — *Sample positioning.*

In order to place the sample cells in the neutron beam each of them was fitted in a holder made from perspex, according to fig. 2.

The cells are thus completely shielded by cadmium foils of 0.3 mm thickness, apart from the aperture of 40 mm diameter determining the diaphragm of the neutron beam through the cell. The apertures have been measured with a travelling microscope to within ± 0.02 mm with the following results :

Sample holder n°	*Diaphragm diameter*
1	(4.006 ± 0.001) cm
2	(4.004 ± 0.002) »
3	(4.001 ± 0.002) »
4	(4.000 ± 0.002) »
(from BCMN Certificate E—42)	

A sample changer, (fig. 3), designed for a positioning accuracy of ± 0.1 mm has four mounting holes fitting the cell holders (ref. 23). This apparatus has the function to interchange automatically, after a preset time, the four samples in the same position of the neutron beam. It was set on the mounting rail of the slow chopper and aligned with the axis of the neutron beam already determined by a flux mapping. Also the windows of the cells were placed perpendicular to the same axis with a precision of ± 0.003 rad. At the same time the flight path length was measured with a telescopic jig adjusted to equal length with the distance between the rotor and the counter bank of the slow chopper. The jig length was measured in the laboratory with a cathetometer. The length of the flight path was, ref. 24,

$$L_o = (194.70 \pm 0.02) \text{ cm.}$$

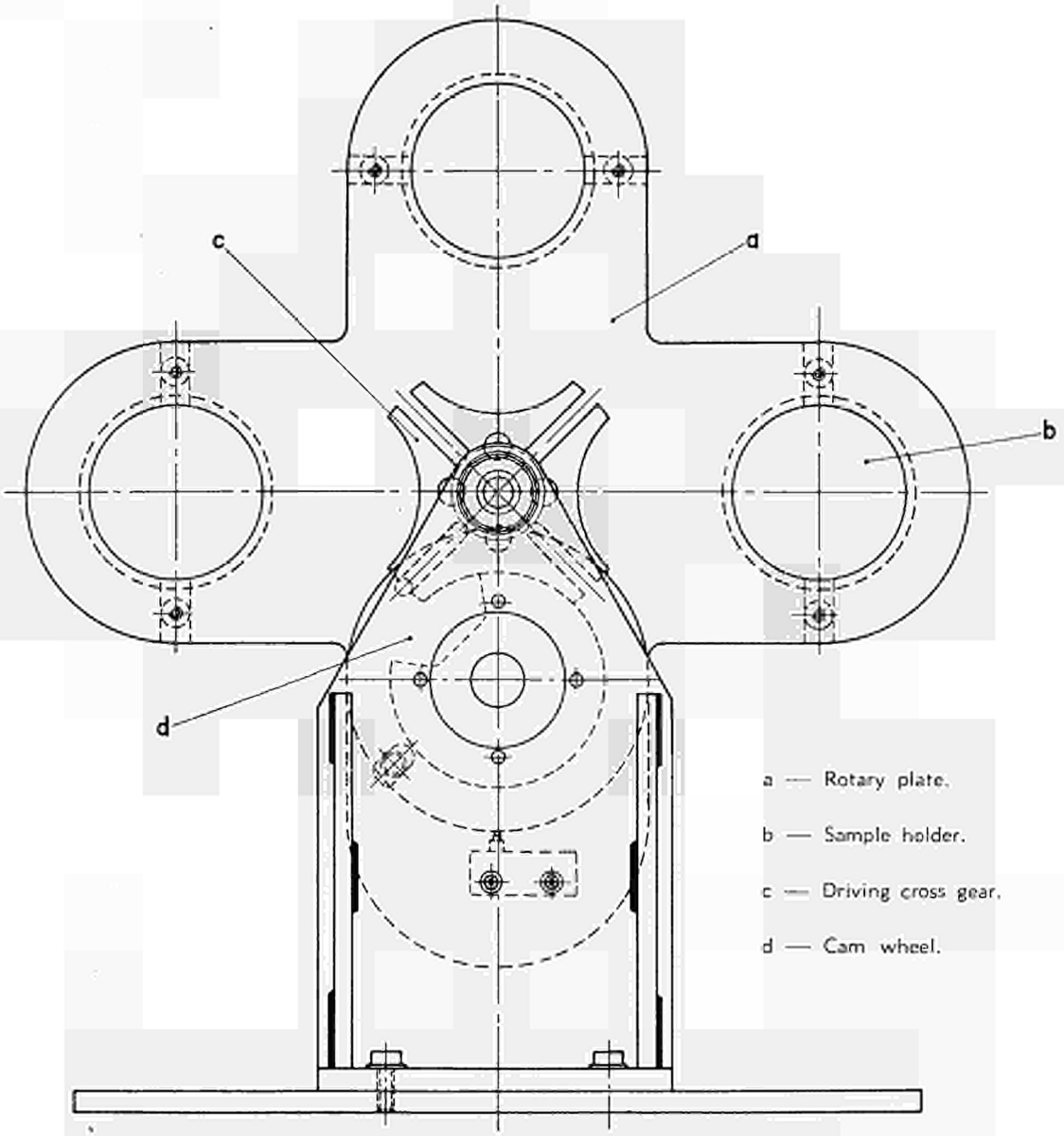

FIG. 3. — Four place sample changer.

3. EXPERIMENTAL APPARATUS. (*)

3.1 — Slow chopper.

3.1.1 — *Rotor.*

The rotor of the chopper is of the well known Fermi type and consists of a stock of plates, alternatively Cd and Al. Each Cd-Al-Cd set forms a neutron transmitting slit, the Al being the slit core and the Cd the walls. The slit width is 1 mm, its length 59 mm, and its

(*) A. J. Deruytter, CEN-SCK.

dimension parallel to the rotation axis is 170 mm. The rotation axis is horizontal. All slits have the same dimensions ; in this way they also have uniform dynamic transmission characteristics, which makes corrections easier.

The chopper is driven by a two-phase asynchronous motor, which is powered by a variable frequency oscillator and output amplifier. Motor speed is variable between 900 and 15.000 revolutions per minute. The stability of this speed over short periods is 0.1 % ; over long periods (several days) 0.5 %.

From the different parameters one derives for the minimum burst time about 20 μs, and for the maximum length of the flight path 2.8 m to avoid overlapping of bursts. In general, however, a flight path of only 2 m is used.

3.1.2 — *Electronic equipment* (ref. 25)

The timing pulses are generated by a 2 MHz quartz oscillator. After passage through a gate, opened by the start signal t_0, the frequency is divided down to 100 kHz, allowing a good precision for the time determination and a minimum channel width of 10 μs. The start signal of the time-base is obtained from a collimated beam of light reflected into a photomultiplier by two mirrors on the rotor axis ; there is a phase difference of 180° between them. Between the start signal and the opening of the first counting channel a delay may be inserted ranging from 0 to 1000 channel widths. Channel widths are provided ranging from 10 μs to 1000 μs in multiples of 10 μs and from 100 μs to 200 μs in multiples of 20 μs.

At the end of the delay period the 25 counting channels are successively opened. Neutron counts arriving during this period are stored in a magnetic core memory. After completion of a measurement, a read-out cycle is generated during which the data are printed out on paper tape. Afterwards a new sample is inserted and a new memory cycle started. All these operations are fully automatic.

3.1.3 — *Detectors.*

The detection system consists of BF_3-counters made by 20th Century Cy., type 12EB70, (1 inch diameter) with their axis perpendicular to the beam direction and at equal distances from the rotor.

3.2 — Neutron energy calibration (ref. 24,26).

For the accurate cross-section work reported here a careful neutron energy calibration was of the utmost importance. So the time of flight of the neutrons from the centre of the rotor to the detectors should be known with good accuracy. To achieve this, the start signal of the timing circuit must exactly coincide with the maximum of the burst intensity at the centre of the rotor ; the distance from the rotor-axis to the detection point of the neutron in the detector and the time elapsed from the start signal to the moment of detection must be determined with care. Possible systematic errors and their influence on the calibration precision are discussed in Appendix III. Here the calibration method is described and the results and final accuracy are discussed.

3.2.1 — *Method.*

To calibrate the wavelength scale we measured the transmission of some polycrystalline materials. They show a sharp break in the coherent scattering cross-section at some typical wave-lengths. This break is broadened by the resolution of the apparatus. Before and after

the break the cross-section varies slowly. For these parts of the transmission curve weighted best straight line fits are calculated. The position of the break is taken at a flight-time such that areas A and B are equal in fig. 4. For a symmetric break this condition yields a flight-time corresponding to a transmission $T_C = \frac{1}{2}(T_A + T_B)$, where T_A and T_B are the transmissions deduced from the extrapolated straight line fits. In both cases of symmetric and non symmetric break the errors on the individual transmission values determine the accuracy of the measured break position. To describe the experimental points a normalized gaussian resolution function :

$$R(t - t') = \frac{1}{a\sqrt{\pi}} \exp\left[\frac{-(t-t')^2}{a^2}\right]$$

was applied with $a = \frac{\Delta t_0}{2\sqrt{\ln 2}}$. Δt_0 is the full width at half height of the resolution function.

To get good transmission values a very stable beam monitor is required. A 4π fission chamber (ref. 27) flow counter with a 0.1 mg/cm² U^{235} — layer was used in the direct beam between the pile collimator and the rotor.

In fig. 4 the cut-off for the (110) planes in α Fe is represented for a rotor speed of 100 revolutions per second. The calculated resolution broadened cut-off for the experimental

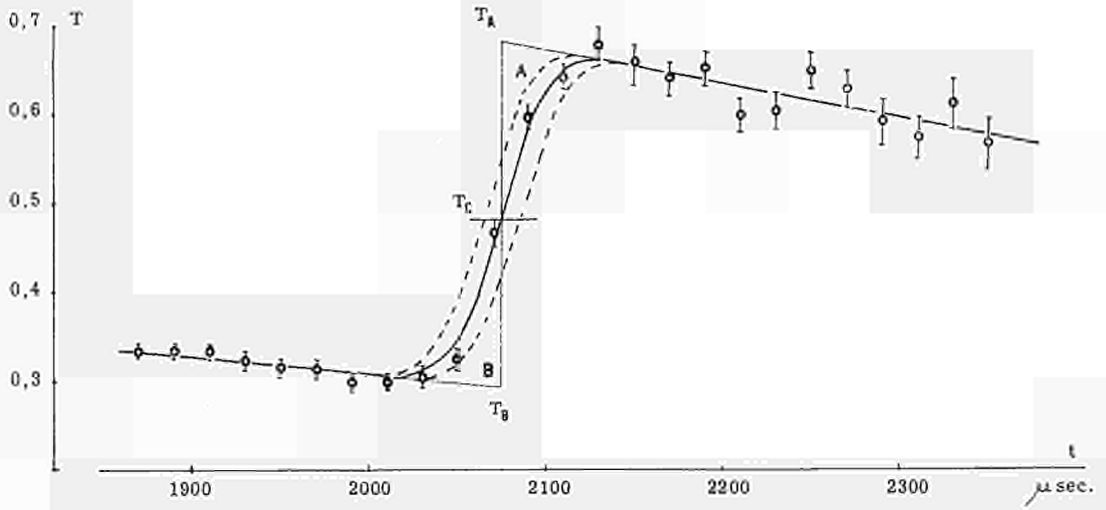

FIG. 4. — Transmission cut-off for the plane (110) of α-Fe.

value of the break-position is shown as a full line. For two fictive break positions shifted over 0.5 % with respect to the determined position, similar curves are shown. The full line fits the experimental points much better. The statistical accuracy of the experimental points is not very high but even then one concludes that errors of 0.2 % can easily be detected.

The accuracy of the method is limited by the statistical errors on the points of the transmission curve for the break considered. A statistical error of 0.2 % for the transmission values seems a reasonable minimum with an acceptable measuring time.

A polycrystal has to be selected with precisely known lattice constants. The accuracy found in crystallographic tables is mostly sufficient. However Gould et and reported a deviation for the graphite break at 6.70 Å of about 0.9 % due to the dependence of the « d »-value of graphite upon the conditions under which it was crystalized. In our graphite sample we did not find such a shift.

For simplicity of analysis a symmetrical break with mean transmission of about 0.5 should be used. Attention should also be paid to the units used for the lattice parameters for there is a difference between them $d_{grating} / d_s = 1.00204$.

Looking at the previously discussed systematical errors and at the error of the calibration method a final total error of 0.2 % was accepted. This was also the mean deviation between the experimental and calculated cut-off positions for several polycrystals as reported in (ref. 26).

3.2.2 — *Calibration measurements for the boron cross-section measurements.*

Before the boron cross section measurements were started, the rotor bearings were replaced. After this operation the light-source PM adjustment was disturbed, so that a delay occured between the start pulse from the PM and the real start pulse of the time base at the moment of maximum neutron intensity at the center of the rotor. During the boron measurements nothing was changed, as this time shift could easily be corrected for by two calibration runs : one in the actual conditions of the boron measurements and one after the proper adjustments were made, (fig. 5).

For these calibration runs the (110)-planes of a sample of α-iron powder were used. The sample has a mean transmission of about 0.5, and the break is almost symmetrical.

Both runs were taken with a different flight-path length :

Run 1 : L = (191.91 ± 0.02) cm,
and Run 2 : L = (194.70 ± 0.02) cm.

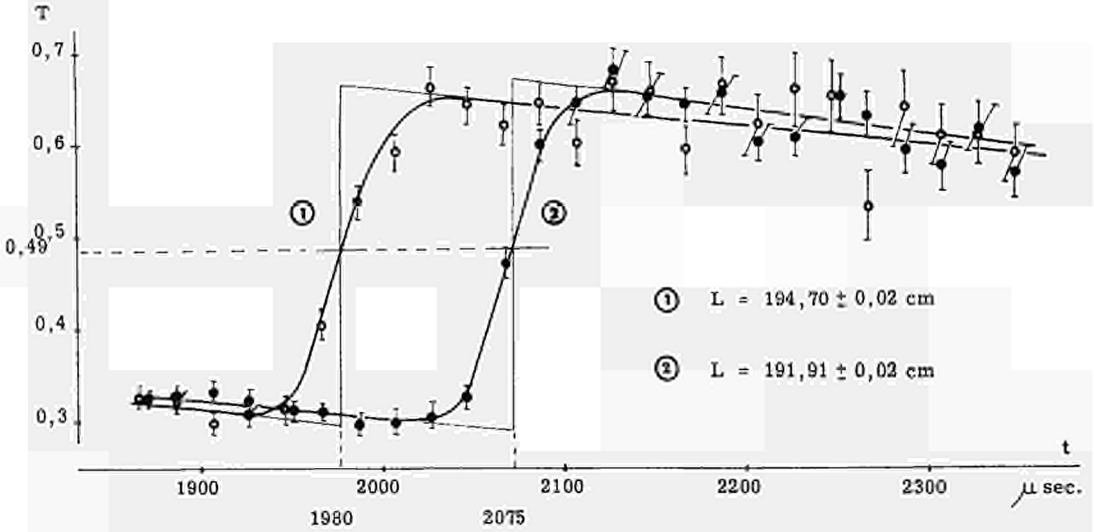

FIG. 5. — Transmission of (110) α-Fe after adjustement (1) and during the boron runs (2).

Both measurements were made with a rotor speed of 100 revolutions per second. The break position was determined as discussed in 3.2.1, and an error of 0.2 % was accepted for both break positions. The time difference between them yields the time shift after correction for the difference in flight-path length.

The result is : t_0-shift = —(123 ± 3) μs. The negative sign means that the total flight time in the boron measurements has to be reduced by this amount.

Some of the boron measurements were made at an other rotor speed. The error however results from an angle difference and should be exactly proportional to the rotor angular speed. In order to check this dependence a graphite sample was run at 50.6 revolutions per second and the shift of the C(002) planes was calculated as —(238 ± 10) μs, in agreement with the previous value assuming angular velocity dependence of the t_0-shift.

4. MEASUREMENTS AND RESULTS (*)

4.1 — Measurement of neutron transmission.

A series of preliminary experiments was performed to check whether some of the experimental conditions are satisfied i.e. :

— the stability of the neutron detectors used as either main time of flight counters (BF_3 proportianal counters) or neutron beam intensity monitors, (4 π geometry fission cham-

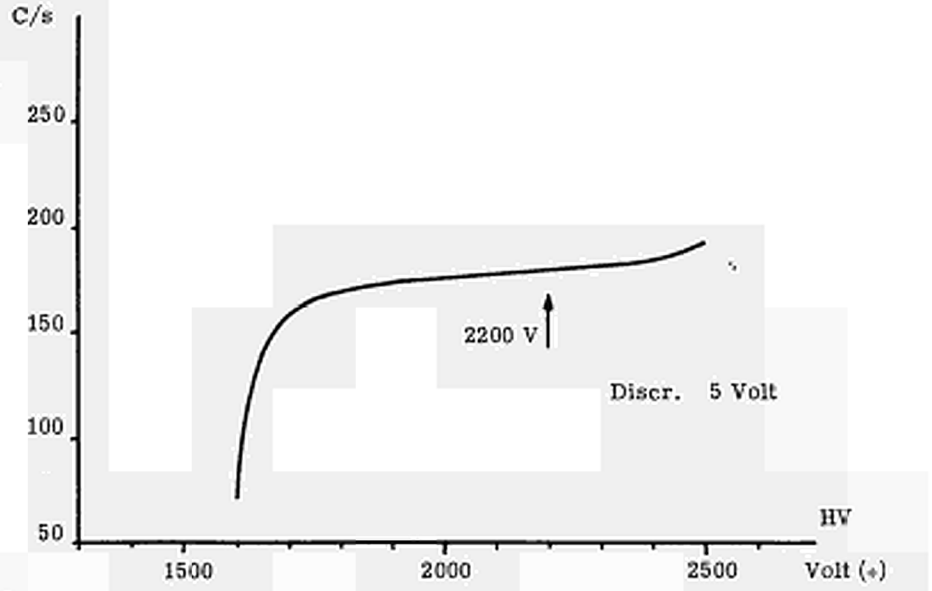

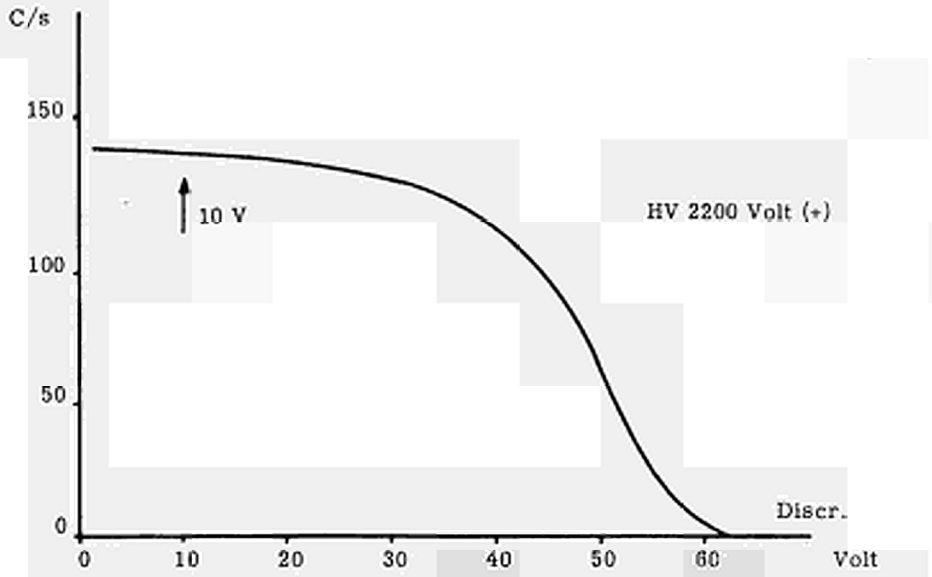

FIG. 6. — BF_3 counters characteristics, (type 12EB70/G).

(*) A. Deruytter, CEN-SCK and A. Prosdocimi, Euratom.

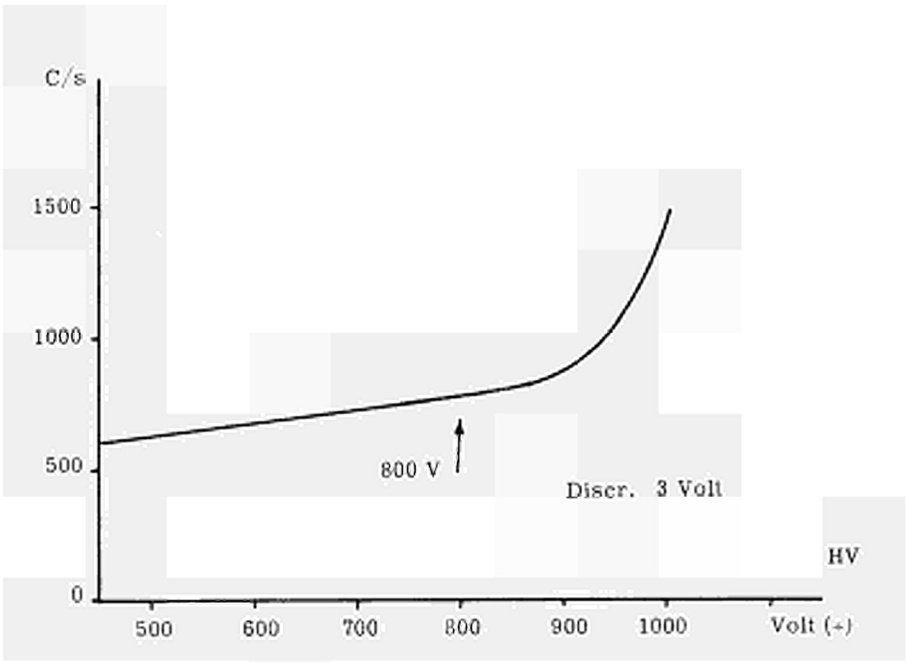

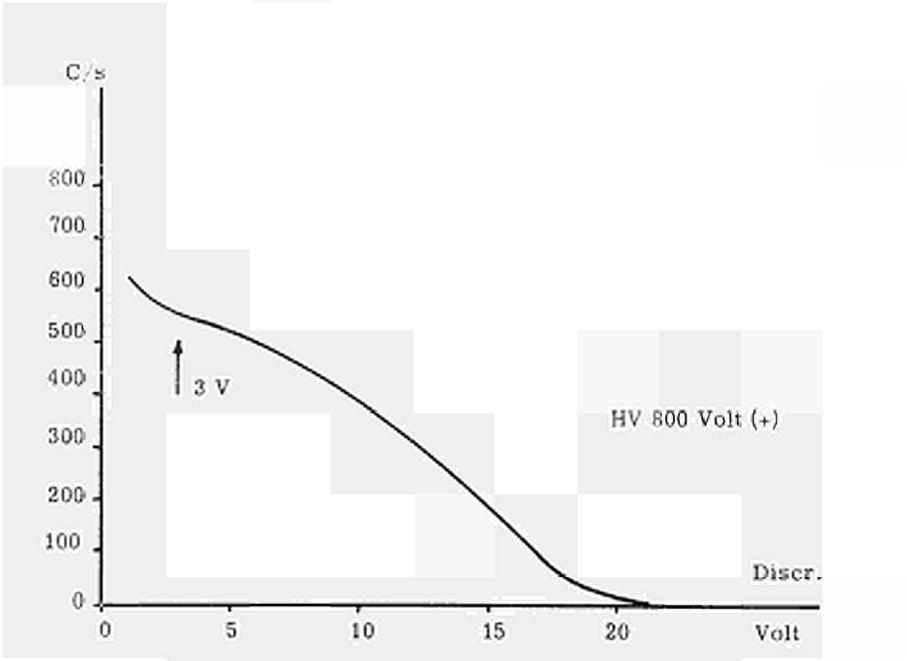

FIG. 7. — U^{235} fission monitor characteristics.

ber). Both of them offer a suitable plateau in the range of working conditions with respect to either the anode voltage or the discrimination threshold (Fig. 6 and 7); the counter readings were repeatedly subjected to tests of statistical acceptability;

— a preliminary transmission test was carried out with samples 8 mm-thick; this proved valuable as a means of defining and improving the measurement conditions, which were found satisfactory when applied to 20 mm-thick test specimens;

— the quartz cells and Cd diaphragms delimiting the effective section of the neutron beam

have been subjected to comparative "blank" transmission tests in order to check their degree of identity and select those most suitable for filling with the boron preparation.

The identical nature of the diaphragms was checked within 0.1 % accuracy, this limit being imposed simply by the statistical counting fluctuations. As a result, a group of five quartz containers proved to be identical to 0.2 % about the mean transmission value for a beam of thermal neutrons

$$\overline{T}=92.5\ \%$$

For each of the samples exposed to the neutron beam, and for every flight time analysis channel, the A counts recorded by the detectors and m counts recorded by the flux monitor were totalised; the two measurements were then repeated placing a 0.5 mm-thick Cd shield in front of the samples, the respective A' and m' count being recorded. This second measurement provides a background count of the thermal neutrons which reach the detector without passing through the test specimen, together with a background count of the epicadmium neutrons ($E>0.5eV$) contained in the beam and counted at their energy or which are slowed on passing through the sample. Accordingly, count normalized to the monitor to be used for the calculations is

$$N = (A/m - A'/m') \qquad [1]$$

or adopting the following quantitative symbols:

Material	*Density*	*Macroscopic Cross-Section*	*Count*	*Thickness*
$B_2O_3+D_2O$ solution	ρ	Σ	N	d
D_2O	ρ_0	Σ_0	N_0	d_0
D_2O in the solution	ρ_1	Σ_1	—	—
B_2O_3 in the solution	ρ_2	Σ_2	—	—
Helium gas	—	—	$\overline{N}$	—

(the macroscopic cross-section of helium is disregarded, being in the ratio of $5 \cdot 10^{-5}$ in relation to that of D_2O), there exist among them the following relations, in which c is the weight concentration of the B_2O_3 in the solution;

$$\rho_1 + \rho_2 = \rho$$

$$c = \rho_2 / (\rho_1 + \rho_2)$$

$$\Sigma_1 + \Sigma_2 = \Sigma$$

$$\Sigma_0 / \Sigma_1 = \rho_0 / \rho_1$$

from which we can derive

$$\Sigma_2 = \Sigma - \frac{\rho}{\rho_0} (1 - c)\ \Sigma_0 \qquad [2]$$

Bearing in mind the proportionality between the neutron current intensity and the detector counts, [1] of 1.3 gives

$$N_0 = \overline{N} \exp\,(-\Sigma_0\, d_0) \qquad [3]$$

$$N = \overline{N} \exp\,(-\Sigma\ d) \qquad [4]$$

thus from [2], [3] and [4] we can derive

$$\Sigma_T\,(B_2O_3) = \Sigma_2 = \frac{1}{d} \ln(\overline{N}/N) - \frac{\rho}{\rho_0}(1-c)\,\frac{1}{d_0} \ln(\overline{N}/N_0) \qquad [5]$$

The total number of counts made per sample and per channel in the course of the two series of measurements, identified by the following "K series" and "L series" symbols, as well as their respective experimental conditions, are given in Tables II and III.

For the two boron solutions, neutron transmission always remained between 32 % and 76 %, values regarded as satisfactory for optimizing the effect of the counting statistics on the error of the result.

The effective number of pulses per channel varies considerably with the position of the channel over the energy range, assuming that for reasons of efficiency the works is carried out at around the peak of the Maxwellian spectrum, the total counts obtained being of the order of 10^3 to 10^5 pulses/channel.

Even the background neutrons were counted in order to be subtracted individually from each channel, their contribution passes from 4 % to 40 % in the case of channels subjected to a less intense flux.

4.2 — Experimental data processing.

As already pointed out in 4.1, each measurement given in Table II is the total of a number of cycles repeated a certain number of times varying from approximately 60 to 80. For each cycle, the time of flight analyser provides the following data :

a) pulses counted by the fission monitor for the whole energy spectrum of the beam impinging on the chopper ;

b) pulses counted by the BF_3 detector and received by the analyser during the analysis time cycle.

c) pulses analysed in each channel of the time of flight analyser.

After a first selection intended to eliminate either incomplete or obviously unreliable results, a second selection was made among the (b) type of counts normalized with respect to the monitor (a), the only ones accepted being those for which the deviation from the average $|x_i - \bar{x}|$, (i being equal to 1, 2... n), has in a normal Gaussian distribution

$$\varphi(x) = \frac{1}{\sqrt{2\pi}} \exp\left[-\frac{1}{2}\left(\frac{x-\bar{x}}{\sigma}\right)^2\right] \qquad [6]$$

a probability $\varphi > 1/2$ n, in which n is te number of times the measurement was repeated (Chauvenet's criterion).

It is only then that the data derived from the time-of-flight analysis (c) were accepted and applied according to formulae [1] and [5] of 4.1 to obtain the macroscopic cross-section of B_2O_3.

The microscopic cross-section of the B_2O_3 molecule is subsequently derived from the relation

$$\sigma_T\ (B_2O_3) = \frac{M}{N_{AV}\ c\ \rho}\ \Sigma_T\ (B_2O_3) \qquad [7]$$

M = molecular mass of B_2O_3
N_{AV} = Avogradro number ($6.02486.10^{23}$ molecules/g mole).

The total cross-section [7] is, according to 1.3, assumed to be a function of the energy, or of the time-of-flight, and expressed as follows :

$$\sigma_T\ (B_2O_3) = (2\,K\tau + 21)\ \text{barn}, \qquad [8]$$

a justifiable hypothesis if the quantity

$$K = \frac{\sigma_T\ (B_2O_3) - 21}{2\,\tau} \qquad [9]$$

proves to be independent of τ.

The values of $\sigma_T\ (B_2O_3)$ as a function of the time-of-flight τ are shown in Table IV for 25 channels of each of the two "K" and "L" series of measurements.

The error $\delta\,\sigma_T$, should be expected to represent the standard deviation of $\sigma_T\ (B_2O_3)$ composed of the corresponding deviations of the directly measures quantities.

According to [5] and [7] of this chapter, $\sigma_T\ (B_2O_3)$ is dependent upon the following quantities : c, ρ_o, ρ, d_0, d, N, N_0 and $\overline{N}$, but only N_0 and N contribute to more than 0.1 % of the error involved in $\sigma_T\ (B_2O_3)$; for this reason, they were taken into account for the calculation of $\delta\sigma_T$.

When we undertook to derive the quantity K from [9], the error contained in the 21 barn and in time of flight τ was also introduced. The first factor cannot be estimated, but as the 21 barn figure constitutes < 2.5 % of the total $\sigma_T\ (B_2O_3)$, the likely error cannot be regarded as affecting δ K to any appreciable extent. The time of flight being determined by.

$$\tau = \frac{t_A + t_0}{L} \qquad [10]$$

t_A = time measured by the analyser
t_o = zero-time calibration
L = flight path.

The error contains either that resulting from the calibration of t_0 given in Table III or that of δL on the flight path.

It should be made clear, however, that δL is mainly determined by the finite dimensions of the neutron detector in the direction of the flight path, Appendix I.

Once the uniformity of K on the 2 x 25 channels measured (Fig. 8), has been determined, the weighted mean value can be derived from it,

$$\overline{K} = \left(\sum_{i=1}^{50} K_i w_i\right) / \sum_{i=1}^{50} w_i \qquad [11]$$

with regard of the statistical weights,

$$w_i = 1 / \delta\ K_i^2 \qquad [12]$$

The corresponding standard deviation is derived from

$$\delta\ \overline{K} = \sqrt{\sum_{i=1}^{50} (K_i - \overline{K})^2\ w_i\ /\ (50 - 1) \sum_{i=1}^{50} w_i} \qquad [13]$$

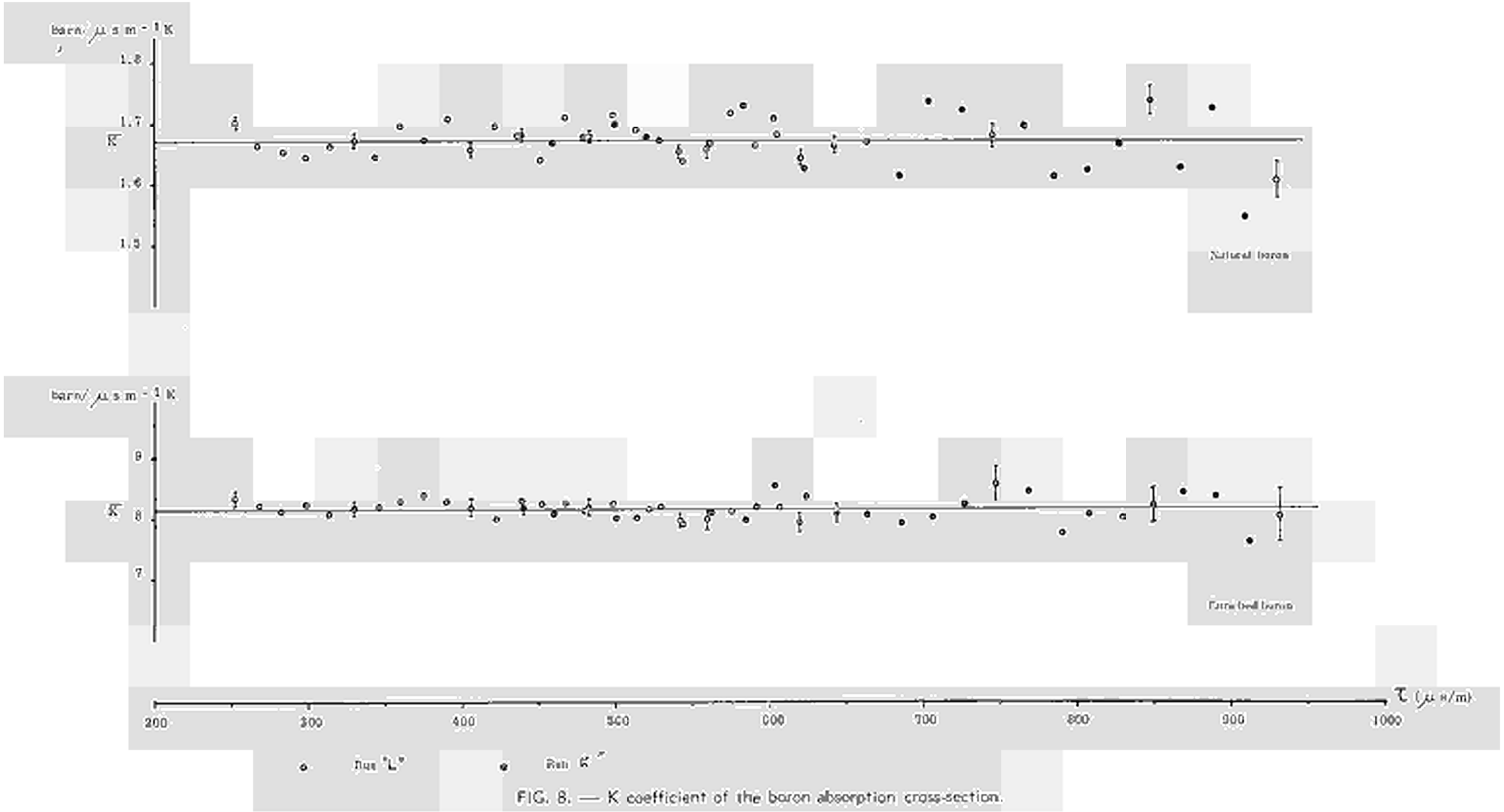

FIG. 8. — K coefficient of the boron absorption cross-section.

4.3 — **Results and Conclusions.**

The development of the above mathematical operations in line with the method expounded in 4.2 leads individually, for the two boron samples with different B^{10} enrichments and in the aggregate for the two series "K" and "L" of measurements, to the following final results :

	$\overline{K} \pm \delta \overline{K}$
Natural boron	1.674 ± 0.0041 barn/μs m^{-1}
Enriched boron	8.15 ± 0.019 barn/μs m^{-1}

The data of paramont significance, however, is the value of σ_A (B) for neutrons travelling at the conventional velocity v_o = 2200 m/s and obtainable from the relation

$$\sigma_A \text{ (B)}_{2200} = \overline{K}/v_o \qquad [11]$$

which after computation gives the following results :

	% B^{10}	σ_A (B) $_{2200}$ barn
Natural boron	19.81 ±0.02	760.8 ± 1.9
Enriched boron	96.515 ± 0.013	3703 ± 8.9

Bearing in mind that the two boron samples differ as to their characteristics, it would be interesting to compare the absorption cross-sections of the B^{10}, σ_A (B^{10}), derived from them, to confirm both the measurement accuracy and the validity of the method involved.

Deduced from	σ_A (B^{10}) at 2200 m/s
Natural boron	3840 ± 11 barn
Enriched boron	3837 ± 9 barn

The agreement between the two results can be regarded as very satisfactory, even when compared, as was the case in Table I, with the best and most recent determinations made.

The weighted mean of both results gives the value for the B^{10} absorption cross-section of (3838 ± 10) barn.

APPENDIX I - FLIGHT PATH DEFINITION (*)

The two extremities of the nominal flight path L_o are located as follows : one on the rotor axis of the chopper provided with rectilinear slits and therefore symmetrical, the other on the geometrical centre of the detector. In view of the fact that the detectors consists of cylinder-shaped BF_3 counters, 2R in diameter, the axis of which is perpendicular to the neutron beam, neutron detection can be carried out at any point of their volume with the probability (see Fig. 9),

$$dp = \Phi\ (x,\ y)\ \Sigma\ dx\ dy \qquad [1]$$

per unit of length of the counter, Σ being the macroscopic cross-section of the filling gas. The neutron flux Φ, owing to its absorption by the counter, varies according to the following law :

$$\Phi\ (x,\ y) = \Phi_0\ \exp\ [\Sigma\ (\sqrt{R^2 - y^2} - x)] \qquad [2]$$

so that, owing to the asymmetry with respect to x, the centre of the moments of the first order of the reactions will be found on an abscissa X which can be calculated in terms of [1] and [2] :

$$X = \int_v x\ dp / \int_v dp = \iint_A x \exp\ [\Sigma\ (\sqrt{R^2 - y^2} - x)]\ dx\ dy / \iint_A \exp\ [\Sigma\ \sqrt{R^2 - y^2} - x)]\ dx\ dy \qquad [3]$$

The value of X, which depends upon the incident neutron energy through Σ, is calculated for each time of flight channel, and serves for correcting the flight path L_o which thus becomes

$$L\ (\tau) = L_0 - X\ (\tau). \qquad [4]$$

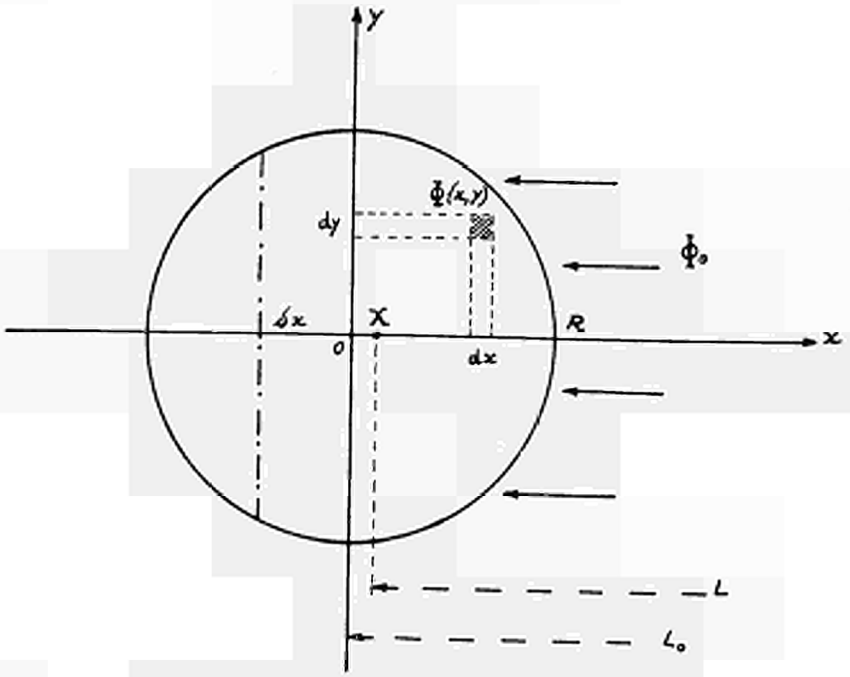

FIG. 9. — Flight path termination in the detector.

(*) A. Deruytter, CEN-SCK and A. Prosdocimi, Euratom.

Owing to the finite size of detectors, the flight path still contains a factor of uncertainty δL, account of which was taken in the time flight error $\delta \tau$ through 4.2 [10].

In order to assimilate this uncertainty factor to an equivalent standard deviation, we assumed, in the simplified case of a uniform flux $\Phi (x, y) = \Phi_0$, that the error on the flight path was the quantity δx, the distance from the axis of the counter limiting the interval within which occur 0.683 of the reactions of the entire counter.

$$\int_0^{\delta x} 4 \sqrt{R^2 - y^2}\, dx = 0.683\, \pi R^2 \qquad [5]$$

In the specific case of 12 E B 70/G counters, the correction of the flight path fell within the interval 0.020 — 0.075 cm.

The error δx which affects the estimation of δL, and indirectly, that of $\delta \tau$, is $\delta x = 0.55$ cm for a cylinder for which $2R = 2.54$ cm.

APPENDIX II - CORRECTION FOR MULTIPLE SCATTERING (*)

Among the incident neutrons removed from the neutron beam as a result of absorption or scattering reactions, some are scattered towards the time-of-flight detector as a result of repeated collisions within the volume of the sample and are analysed together with those transmitted. In order to estimate the probability of such phenomena we used a simplified model, the scope of which was confined to the study of monokinetic neutrons which penetrate into the

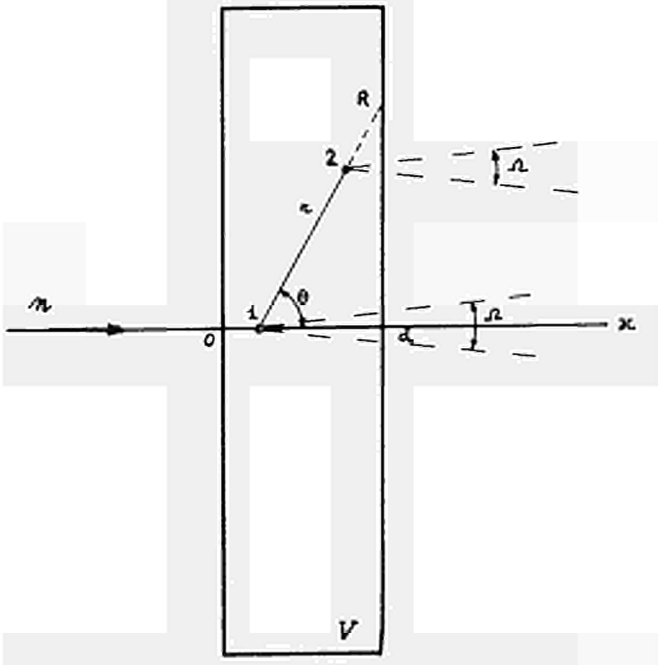

FIG. 10. — Multiple collisions inside the sample.

(*) A. Prosdocimi, Euratom.

sample along its axis and, once inside, undergo a process of isotropic scattering not involving any energy exchange. The probability P_1 that an incident neutron, after a first collision at point 1 (fig. 10) is scattered and transmitted into the solid angle Ω is

$$P_1 = \frac{\Omega}{4\pi} \int_0^d \exp.\ (-\Sigma x)\ .\ \Sigma_s\ .\ \exp\ [-\Sigma\,(d-x)]\ dx =$$

$$= \frac{\Omega}{4\pi}\ \Sigma_s d\ \exp\ (-\Sigma d) \qquad [1]$$

The probability P_2 that the above process will occur after a second collision at point 2 subsequent to the first one is made up of the various probabilities which must be integrated within the entire volume V of the test specimen :

$$P_2 = \frac{\Omega}{4\pi} \int_V [\exp\ (-\Sigma x)\ \Sigma_s\ .\ dx]\ .\ \left[\frac{1}{2}\sin\theta\ d\theta\right]$$

$$.\ [\exp\ (-\Sigma r)\ \Sigma_s\ dr]\ .\ [\exp\ [-\Sigma\ (d\text{-}x\text{-}r\cos\theta)]] =$$

$$= \frac{\Omega}{8\pi} \sum_s^2 \exp\ (-\Sigma d) \int_0^d dx \int_0^\pi \sin\theta\ d\theta \int_0^{R(x,\theta)} \exp\ [-\Sigma r\ (1-\cos\theta)]\ dr \qquad [2]$$

The calculation of the probability for scattering of the order > 2 proves to be extremely complicated ; accordingly, we shall confine ourselves to the first two terms of the total probability $P = P_1 + P_2 + \ldots + P_i + \ldots$, particularly since higher order probabilities grow more and more remote.

If we pass on to the numerical treatment of the special cases in which two samples are filled with heavy water and a B_2O_3 solution respectively, at a neutron energy of 0.0253 eV, and having the following characteristics :

$\Sigma_S\ (D_2O) = \Sigma_S$ solution $=$ 0.449 cm^{-1}
$\Sigma\ (D_2O) =$ 0.449 »
Σ (solution) 0.711 »
$d = 2$ cm
$\Omega/4\pi = 10^{-3}$

we can derive directly from [1], and by means of numerical integration from [2].

	D_2O	$D_2O + B_2O_3$
P_1	0.00037	0.00011
P_2	0.00039	—

Results of the same order of magnitude would be found if more stringent theoretical treatments were applied ; thus, the probability P for an infinite diffusing flat layer would be, according to ref. 28, 29 and 30 :

	D_2O	$D_2O + B_2O_3$
P	0.00082	0.00021

Whatever results are deemed to be more acceptable, values of P are small enough to be disregarded as compared with the other errors affecting the present measurements, particularly since the effect which they have in transmission experiments is determined by the difference between their values for heavy water and the boron solution respectively.

APPENDIX III - SYSTEMATIC ERRORS (*)

1. The start signal t_o :

a) *Phase shift with respect to the crystal pulses :* The timing pulses are generated by a 2 MHz quartz oscillator. With this high frequency, the error due to the randomness of phase of the start signal and the 2 MHz pulses is reduced to a maximum of 0.5 μs.

b) *Sensitivity to the PM pulse width.* The relatively broad PH pulse passes through a differentiating circuit yielding a sharp start pulse at the maximum of the PM pulse. But with different rotor speeds, ranging from 50 to 250 revolutions per second, the width of the PH pulse will change and the differentiating circuit is somewhat sensitive to this width. In this way shifts of 0.5 μs may occur.

c) *Parallelism of both mirrors and adjustment of the coincidence between PM pulse and burst.*

For reasons of intensity we wanted two bursts per revolution ; so two parallel mirrors were necessary. To minimize this correction, an end-gauge was fixed in the rotor-axis, with thickness variations over the whole surface smaller than ± 0.02 μ, yielding a parallelism between the two planes better than 1 second of arc. By rotating the rotor over 180° no corrections were necessary to the light source PM adjustment. The adjustment of the coincidence between burst and maximum of the PM pulse is limited by the mechanical finish of the positioning mechanism of the lamp with respect to the PM, and by the accuracy of the determination of the maximum intensity in the detectors. In this way the precision of the t_0-determination is smaller than 2 minutes of arc, a smaller than 0.5 μs/m with a rotor speed of 100 revolutions per second. The mechanism we used could certainly be improved, and the error reduced.

2. Length of the flight-path : length measuring technique and shift of the mean detection point.

a) The end point of the flight-path is the detection point of the neutron. 12 EB 70/BF_3-counters with a 1 inch diameter are used. The mean detection point does not coincide with the central wire, but is shifted towards the coming neutrons. This shift is a function of the neutron energy and typical figures are $E_n = 0.025$ eV, shift = 0.04 cm.

(*) A. J. Deruytter, CEN-SCK.

b) To measure the length of the path a telescopic system was used, provided with a disk at one side and a threaded head at the other. The disk, perpendicular to the rod, served as a tangent plane to the rotor. At the other side a metal plate with accurately known thickness was put tangent to the counters. By the threaded head the system length was adjusted to the distance from rotor to counters and measured afterwards in the laboratory to $\pm$ 0,1 mm. From the knowledge of the rotor diameter and the shift of the mean detection point the mean length can be determined for each neutron velocity with a precision of about 0.2 mm. For the 2 m flight path this measuring technique yields an error of about 10^{-4}.

Due to the finite thickness of the BF_3-detectors there is a distribution of individual path-lengths about the used mean length. This distribution influence the resolution, but does not have a great effect on the calibration of the wavelength-scale, as there is a good agreement between experimental and theoretical resolution widths. For the cut-off of the (110)-planes in α Fe (See Fig. 4) the experimental resolution width is 52 μs. The theoretical width is 50 μs calculated from burst duration, channel width, mean thickness of the counters, etc., in the usual way. Both are in very good agreement.

3. Time of arrival.

The pulse from the BF_3-counter allows the measurement of the elapsed time. By means of a pulse-shifter this pulse is shifted towards the following clock-pulse. The BF_3-pulse only passes through this circuit upon arrival of the following 10 μs pulse. The full width at half heighth of the clock pulse is 0.25 μs. The rise time of the BF_3-pulse after amplification and discrimination is about 0.8 μs. The pulse-shifter is adjusted so as to give an output-signal when the BF_3-pulse reaches half its height when coincident with the clock pulse. So the BF_3-pulse should arrive at least 0.4 μs before the end of the clock pulse in order to be counted in the right channel and not be shifted towards the following clock pulse. This means a 0.15 μs-shift towards long wavelengths. An improvement would be possible by the use of fast transistorized equipment, or by using the 0.1 μs fast scintillation time in a ZnS-B^{10} counter.

4. Elapsed time.

The frequency of the crystal, used as a master oscillator for the timing circuits, was established as 20° C as 2,000,203.6 $\pm$ 0.1 Hz, and the temperature dependence of the frequency was determined as —0.4 Hz/°C by C.C.R.M. (Centre de Contrôle des Radiocommunications des Services Mobiles, Uccle, Belgium). So the time frenquency equals 2 MHz within 10^{-4}, an order of magnitude smaller than the final error in the flight time.

In the following table a list of the systematic errors is given with their absolute value and their relative error in the time-of-flight. The calculations are made for 500 μs/m neutrons, 100 rps rotor speed and a 2m flight-path.

Source of Error	*Absolute Value*	*Relative error in the time-of-flight*
1) Start Signal.		
a) Phase shift with respect to the crystal pulses	0.5 μs	5×10^{-4}
b) Sensitivity of differentiation circuit to the PM pulse width	0.5 μs	5×10^{-4}
c) Parallelism of both mirrors	1 second of arc (0.01 μs)	10^{-5}
	2 minutes of arc (1 μs)	10^{-3}
2) Length of the flight path. Shift of the mean detection point and the length measuring technique	0.2 mm	10^{-4}
3) Time of arrival. Rise time of the detector pulses and width of the clock pulses	0.15 μs	1.5×10^{-4}
4) Elapsed time. Deviation of the crystal frequency from 2 MHz	203.6 ± 0.1 Hz (0.1 μs)	10^{-4}
Temperature dependence of the frequency .	—0.4 Hz/°C (2×10^{-3} μs)	2×10^{-6}
Total error due to systematic errors		1.3×10^{-3}

REFERENCES

1 — EGELSTAFF P. A. — AERE Memorandum N/M 62 (1953).

2 — HAMERMESH B., RINGO G. R., WEXLER S. — Phys. Rev. **90**, 603 (1953), mentioning unpublished results by Kimball, Ringo, Robillard and Wexler.

3 — CARTER R. S., PALEVSKY H., MYERS V. W., HUGHES D. J. — Phys. Rev. **92**, 716 (1953).

4 — GREEN A, LITTLER D. J., LOCKETT E. E., SMALL V. G., SPURWAY A. H., BOWELL E. — Jour. Nucl. Ener. **1**, 144 (1954).

5 — SCOTT F. R., THOMSON D. B., WRIGHT W. — Phys. Rev. **95**, 582 (1954).

6 — COLLIE C. H., MEADS R. E., LOCKETT E. E. — Proc. Phys. Soc. A **69**, 464 (1956).

7 — EGELSTAFF P. A. — Jour. Nucl. Ener. I **5**, 41 (1957).

8 — HAVENS W. W., MELKONIAN E., RUSTAD B. — Report CU - 160 (1957).

9 — von DARDEL G., SJOESTRAND N. G. — Phys. Rev. **96**, 1566 (1954).
von DARDEL G., SJOESTRAND N. G. — Progr. Nucl. Energ., vol. **2**, 216 (1958).

10 — IGNATEV, KIRPICHIKOV, SUKHORUCHKIN — Proc. Int. Conf. on Peaceful Uses of Atomic Energy 1958, vol. **16**, 209.

11 — SCHMITT H. W., BLOCK R. C., BAILEY R. L. — Nucl. Phys. **17**, 109 (1960).

12 — SAFFORD G. J., TAYLOR T. I., RUSTAD B. M, HAVENS W. W. Jr — Phys. Rev. **119**, 1291 (1960).

13 — GOULD F. T., TAYLOR T. I., HAVENS W. W. Jr., RUSTAD B. M., MELKONIAN E. — Nucl. Sci. Eng. **8**, 453 (1960).

14 — DEBUS G., DERUYTTER A., LAUER K., MORET H., PROSDOCIMI A., — this report.

15 — SAFFORD G. J., TAYLOR T. I., RUSTAD B. M., HAVENS W. W. Jr. — Nucl. Sci. Eng. **9**, 99 (1961).

16 — HUGHES D. J. — Proc. Int. Conf. on Peaceful Uses of Atomic Energy 1958, vol. **16**, 8.

17 — HUGHES D. J., SCHWARTZ R. B. — Neutron Cross Sections BNL-325, 2nd ed. and Suppl. (1958).

18 — TITTMAN J., SHEER C. — Phys. Rev. **83**, 746 (1951).

19 — LAUER K. F., LE DUIGOU Y. — Z. Anal. Chem., **184**, 4 (1961).

20 — FINCK C., KLEINBERGER R. et al. — J. Nuclear Energy, **3**, 25 (1956).

21 — SPAEPEN J. — Meded. Kon. Vlaam. Akad. Wetensch. Belg. **19**, no. 5 (1957).

22 — MORET H. — Rev. Sci. Instr., to be published.

23 — MORET H. — Nucl. Instr. and Meth., **14**, 2 (1962).

24 — CEULEMANS H., DERUYTTER A., MORET H., NEVE DE MEVERGNIES M. — Symposium on Time-of-flight Methods, Paris 1961, p. 275.

25 — CEULEMANS H., DEKEYSER A., MIES E. — L'Electronique Nucléaire, vol. 2, 297, Paris (1959).

26 — CEULEMANS H., DERUYTTER A. J. — Symposium on Pile Neutron Research, IAEA, Vienna (1960) ; and CEN-SCK Report R-1900.

27 — DERUYTTER A. J. — Nucl. Instr. and Meth., **7**, 145 (1960).

28 — VINEYARD G. H. — Phys. Rev., **96**, 93 (1954).

29 — CHANDRASEKHAR S. — Radiative Transfer, Oxford (1950).

30 — CHANDRASEKHAR S., ELBERT and FRANKLIN — Astrophys. J. **115**, 244 (1952) and **115**, 269 (1952).

Tab. I — STATUS OF MEASUREMENTS

Ref.	Year	Laboratory	Method	Energy, eV
1	1953	AERE-Harwell	Transmission by slow chopper	0.01 - 0.1
2	1953	ANL - Argonne	Transmission	
3	1953	BNL - Brookhaven	Transmission by slow chopper	0.0003 - 0.04
3	1953	BNL - Brookhaven	Transmission by slow chopper	0.0008 - 0.04
4	1954	AERE-Harwell	Pile oscillator with reference to gold	thermal spectrum
5	1954	LASL-Los Alamos	Neutron lifetime	
6	1956	Oxf. Un.-Oxford	Neutron lifetime	
6	1956	Oxf. Un.-Oxford	Pile oscillator with reference to measured boron	
7	1957	AERE-Harwell	Transmission by slow chopper	0.01 - 0.1
7	1957	AERE-Harwell	Transmission by slow chopper	0.01 - 0.1
8-13	1957	Col. Un.-New York	a) Chrystal spectrometer b) Pulsed cyclotron	0.0006 - 1 0.012 - 0.12
9	1958	AE-Stockholm	Neutron lifetime	
9	1958	AE-Stockholm	Neutron lifetime	
10	1958	USSR	Transmission by pulsed cyclotron	
11	1960	ORNL-Oak Ridge	Transmission by fast chopper	0.018 - 0.4
11	1960	ORNL-Oak Ridge	Transmission by fast chopper	0.022 - 0.042
12	1960	Col. Un.-New York	Transmission by crystal spectrometer	0.00291 - 0.1
12	1960	Col. Un.-New York	Transmission by crystal spectrometer	
14	1961	CEN-BCMN - Mol	Transmission by slow chopper	0.006 - 0.08
14	1961	CEN-BCMN - Mol	Transmission by slow chopper	0.006 - 0.08

Sample	Boron source - Isotopic ratio	2200 m/s cross-section barn	Value normalized to B^{10} barn
Quartz cell containing D_2O+NaOD solution of B_2O_3	natural	781 ±10	3898± 63
	ANL standard boron	755 ± 3	3813± 40
Aluminium cell containing D_2O solution of B_2O_3	California boron by ANL	749 ± 4	3782± 42
Boron glass plates manufactured by Corning Glass Co.	California boron	752 ±13	3797± 75
Heavy water solution of B_2O_3	Harwell standard boron	785 ± 8	3914± 57
	California boron	744 ±20	3757±107
Water solution of borax	natural	761 ± 2	—
	Harwell standard boron	760 ± 3	3792± 42
Quartz cell containing D_2O+NaOD solution of B_2O_3	Harwell standard boron	771 ± 5	3847± 47
Boron glass powder	Harwell standard boron	769 ± 5	3837± 47
Boron glass plates manufactured by Corning Glass Co.	California boron	756 ± 6	3818± 48
Water solution of borax	natural	758 ± 4	—
Water solution of borax	ANL-BNL standard boron	760 ± 4	3838± 20
	natural	757.5± 3.5	—
Aluminium cell containing D_2O solution of B_2O_3	enriched boron (result reduced to B^{10})	—	3848± 38
	ANL-BNL standard boron 19.8 % B^{10}	753 ± 6	3803± 48
Quartz cell containing D_2O solution of $NaBO_2$	enriched boron (result reduced to B^{10})	—	3838± 11
Quartz cell containing D_2O solution of $NaBO_2$	ANL-BNL standard boron	764 ± 3	3858± 25
Quartz cell containing D_2O solution of deuterated boric acid	natural, 19.81 % B^{10}	760.8± 1.9	3840±11
Quartz cell containing D_2O solution of deuterated boric acid	enriched, 96.51 % B^{10}	3703 ± 9	3837± 9

Tab. II — COUNTING IN THE TIME-OF

Run	Channel	Natural boron sample		Enriched
		A	A'	A
"K„	Monitor	28858090	9610550	36961710
	1	53430	967	64008
	2	48561	924	58256
	3	41863	882	50280
	4	34078	971	40839
	5	27158	833	32284
	6	22550	806	26880
	7	18527	800	22045
	8	16733	770	20434
	9	16752	761	19524
	10	15581	678	18072
	11	13225	678	15644
	12	11133	674	12998
	13	9097	616	10664
	14	7238	649	8521
	15	6807	613	8020
	16	6394	549	7271
	17	5693	550	6412
	18	5130	467	6038
	19	4607	445	5485
	20	4164	442	4847
	21	3660	437	4212
	22	3190	369	3602
	23	2705	347	3235
	24	2373	303	2788
	25	2063	285	2368
"L„	Monitor	44330570	9144485	47039965
	1	113373	945	115000
	2	119811	993	121426
	3	118211	992	119980
	4	114379	963	115519
	5	108051	977	109589
	6	101096	976	102235
	7	96380	945	96619
	8	89209	976	89917
	9	82633	888	81914
	10	78700	918	79134
	11	74052	876	73683
	12	66846	887	67417
	13	59549	796	58875
	14	53909	753	53192
	15	49512	781	49244
	16	43725	722	43329
	17	36661	675	36480
	18	30965	670	30726
	19	25993	623	25506
	20	22720	589	22351
	21	19422	548	19153
	22	16760	519	16674
	23	17247	510	16807
	24	16209	448	15926
	25	15307	411	15034

boron sample	Heavy water blank		Helium blank	
A'	A	A'	A	A'
10367630	29934400	8641810	22772360	8658310
1013	87940	924	171302	1635
972	81371	914	156970	1628
976	71592	833	136860	1458
893	59013	813	117159	1470
888	47948	808	97305	1442
825	39996	752	81545	1355
840	33320	742	68886	1313
813	31290	716	65666	1164
841	31578	651	67435	1189
822	29627	717	64718	1124
744	25588	669	57047	1105
674	21595	624	48293	1009
645	17505	606	40039	1007
610	14173	576	32742	915
620	13471	535	31349	922
600	12764	504	29917	837
537	11469	493	27243	828
490	10334	435	25685	731
516	9483	443	23551	711
452	8574	394	21150	657
421	7586	353	19040	590
398	6500	315	16583	560
386	5788	318	14346	493
326	4738	275	12466	435
297	4188	253	10630	425
8523420	41203860	8464320	35802625	7682195
849	137485	923	273899	1334
884	147776	978	295795	1441
890	147883	976	297024	1452
907	145088	936	294146	1543
895	139765	980	286229	1524
917	133055	975	278824	1556
908	128319	992	266937	1522
918	121512	950	253876	1474
864	113615	826	239393	1419
848	111027	909	234390	1375
765	104683	836	223598	1380
753	96309	760	207072	1279
693	87138	751	188084	1222
720	79781	777	174417	1112
680	75426	748	163830	1185
649	66846	704	148055	1076
620	57424	678	127558	989
560	48390	629	110091	942
562	40936	609	93745	907
511	35694	558	83538	793
482	30993	511	72451	804
461	27474	468	64822	794
466	28350	477	67754	701
425	27335	417	66546	655
379	25993	402	64090	633

Tab. III — EXPERIMENTAL CONDITIONS FOR THE SLOW CHOPPER

	Run « K »	Run « L »
Rotor speed	75.18 ± 0.09 rps	100.24 ± 0.22 rps
Neutron burst length (full width)	71 μs	53 μs
Delay time, t_A	1000 μs	1000 μs
Channel width	40 μs	30 μs
Zero-time calibration	— (165 ± 4) μs	— (123 ± 3) μs
Counting time	1000 s/cycle	1000 s/cycle
Useful cycles	58 - 66	78 - 83
Flight path, L_0	194.70 ± 0.02 cm	

Tab. IV. — BORON TOTAL CROSS-SECTION VERSUS TIME-OF-FLIGHT

Run	Channel n°	τ μs/m	Natural boron		Enriched boron	
			σ_T (B_2O_3) barn	$\delta\sigma_T$ (B_2O_3) barn	σ_T (B_2O_3) barn	$\delta\sigma_T$ (B_2O_3) barn
" L "	1	252,47	860,10	4,40	4200,74	55,99
	2	267,88	913,15	4,25	4434,04	57,90
	3	283,29	958,78	4,27	4613,28	58,24
	4	298,70	1004,18	4,32	4925,88	59,33
	5	314,11	1065,70	4,47	5092,70	61,15
	6	329,53	1124,05	4,64	5396,58	63,70
	7	344,94	1155,65	4,76	5673,72	65,71
	8	360,35	1242,57	4,97	5958,44	68,51
	9	375,77	1277,21	5,13	6324,45	71,43
	10	391,18	1356,44	5,31	6467,11	73,04
	11	406,59	1368,62	5,47	6634,83	75,20
	12	422,00	1451,57	5,80	6759,40	79,10
	13	437,42	1489,88	6,16	7224,74	85,00
	14	452,83	1506,81	6,52	7462,13	91,45
	15	468,25	1622,47	6,89	7749,32	95,10
	16	483,66	1645,70	7,41	7893,66	102,8
	17	499,08	1731,44	8,25	8233,67	114,9
	18	514,49	1759,06	9,29	8257,88	127,4
	19	529,91	1792,22	10.44	8690,09	146,9
	20	545,32	1806,28	11,00	8640,06	153,8
	21	560,74	1879,48	12,60	8947,87	175,8
	22	576,15	2001,54	13,86	9359,12	193,4
	23	591,57	1989,32	13,48	9689,45	192,0
	24	606,98	2062,24	13,52	9944,91	193,3
	25	622,40	2065,16	13,81	9893,67	195,9
" K "	1	439,27	1498,16	5,992	7215,86	77,93
	2	459,82	1554,33	6,320	7442,99	82,00
	3	480,37	1632,37	6,844	7812,54	89,43
	4	500,93	1721,84	7,883	8028,82	101,1
	5	521,48	1769,48	8,969	8533,05	117,8
	6	542,03	1813,67	10,12	8629,10	132,2
	7	562,59	1895,03	11,65	9062,32	153,4
	8	583,14	2038,64	12,36	9294,08	160,6
	9	603,70	2083,46	12,26	10308,93	165,0
	10	624,25	2049,08	12,46	10443,57	172,5
	11	644,80	2163,76	14,30	10430,98	191,6
	12	665,36	2242,47	16,40	10744,56	216,6
	13	685,92	2231,99	19,03	10866,00	255,4
	14	706,47	2478,31	24,00	11337,62	307,6
	15	727,03	2527,20	24,73	11949,37	328,3
	16	747,59	2533,87	25,09	12819,44	354,0
	17	768,14	2626,35	28,08	12961,20	381,8
	18	788,70	2566,31	28,40	12253,40	387,7
	19	809,26	2646,62	31,34	13021,22	445,3
	20	829,82	2784,81	32,12	13309,04	469,5
	21	850,38	2982,47	39,67	13989,64	525,7
	22	870,93	2852,47	41,84	14701,93	614,0
	23	891,50	3096,02	49,08	14905,06	645,7
	24	912,05	2840,97	52,76	13883,37	744,2
	25	932,61	3020,52	60,23	14976,65	858,6

CDNA00012ENC